Numerical solution of Cauchy problems in linear elasticity in axisymmetric situations

Bastien Durand [a,b], Franck Delvare [a,*], Patrice Bailly [a]

[a] Institut PRISME, ENSI de Bourges, F-18020 Bourges Cedex, France
[b] CEA, DAM, Le Ripault, F-37260 Monts, France

ARTICLE INFO

ABSTRACT

An iterative method for solving axisymmetric Cauchy problems in linear elasticity is presented. This kind of problem consists in recovering missing displacements and forces data on one part of a domain boundary from the knowledge of overspecified displacements and forces data on another part of this boundary. Numerical simulations using the finite element method highlight the algorithm's efficiency, accuracy and robustness to noisy data as well as its ability to deblur noisy data. An application of the inverse technique to the identification of a friction coefficient is also presented.

© 2011 Elsevier Ltd. All rights reserved.

1. Introduction

Inverse problems can be defined by opposition to direct problems (Kubo, 1988) and characterized by the lack of knowledge of one of the following elements of information: the geometry of the domain, the equilibrium equations, the constitutive equations, the boundary conditions on the whole boundary of the domain and the initial conditions. According to this definition, many mechanical problems, for instance, identification of material parameters, identification of unknown boundaries (such as cracks or cavities), identification of initial boundary conditions, identification of inaccessible boundary conditions can be considered as inverse problems and more specific examples relating to elasticity problems can be found in Bonnet and Constantinescu (2005).

In a mathematical sense, direct problems can be considered as well-posed problems. In linear cases, these problems have a unique solution which is stable (continuously dependent on the data). Conversely, inverse problems are generally ill-posed problems in the Hadamard sense (Hadamard, 1923), since the existence or uniqueness or the continuous dependence on the data of their solutions may not be ensured.

This paper examines, in axisymmetric situations, an inverse boundary value problem in linear elasticity, namely known as a Cauchy problem. It consists in recovering missing displacement and force data on some part of the boundary of a domain from overspecified displacement and force data on another part. In this case, the equilibrium equations, the constitutive equations, the domain and its boundary are known.

In order to solve Cauchy problems in linear elasticity, many regularization methods have been introduced which can be classified as Tikhonov type methods (Bilotta and Turco, 2009; Koya et al., 1993; Maniatty et al., 1989; Marin and Lesnic, 2002a, 2003, 2004; Marin, 2005; Schnur and Zabaras, 1990; Tikhonov and Arsenin, 1977; Yeih et al., 1993; Zabaras et al., 1989) or iterative methods (Andrieux and Baranger, 2008; Delvare et al., 2010; Ellabib and Nachaoui, 2008; Marin, 2009; Marin et al., 2001, 2002b; Marin and Lesnic, 2005; Marin and Johansson, 2010a,b) Tikhonov regularization methods present the advantage of leading to well-posed problems where the equilibrium equations have been modified. Some iterative methods are based on the use of a sequence of well-posed problems and others on the minimization of an energy-like functional. Numerical algorithms are implemented using different numerical methods, such as the finite element method (FEM) (Andrieux and Baranger, 2008; Bilotta and Turco, 2009; Delvare et al., 2010; Maniatty et al., 1989; Schnur and Zabaras, 1990), the boundary element method (BEM) (Ellabib and Nachaoui, 2008; Koya et al., 1993; Marin et al., 2001, 2002a,b; Marin and Lesnic, 2002a,b, 2003, 2005, 2010a; Marin, 2009; Yeih et al., 1993; Zabaras et al., 1989) or meshless methods (Marin and Lesnic, 2004; Marin, 2005; Marin and Johansson, 2010b). Some papers present comparisons between different numerical methods (Marin et al., 2002a; Marin, 2009).

---

* Corresponding author.
  E-mail address: franck.delvare@ensi-bourges.fr (F. Delvare).

A somewhat different resolution approach was introduced in Cimetière et al. (2000, 2001), Delvare et al. (2002) to solve the Cauchy problem for the Laplace equation and was extended to solve the Cauchy problem in linear elasticity by Delvare et al. (2010). This approach reduced the resolution of the Cauchy problem to the resolution of a sequence of optimization problems under equality constraints. The functional is composed of two terms. At each step of the resolution, the first term (relaxation term) gives the gap between the optimal element and the overspecified boundary data, the second one (regularization term) gives the gap between the optimal element and the previous optimal element. The equality constraints are the equilibrium equations. So, at each step an optimal element is obtained which is an exact solution to the equilibrium equations and is nearer to the overspecified data than the previous optimal element calculated. In the case of compatible data, it was also proved that the sequence converges and its limit is the solution to the Cauchy problem. The additional regularization term tends to zero as its iterations continue.

In this paper, this inverse technique is extended to solve axisymmetric Cauchy problems in linear elasticity. Section 2 is devoted to the formulation of the Cauchy problem in linear elasticity in axisymmetric situations. Section 3 describes the iterative inverse method and Section 4 is devoted to its numerical implementation using the finite element method. In Section 5, several numerical simulations are presented and in Section 6, the application of the method to the identification of the friction coefficient is presented.

2. The Cauchy problem in linear elasticity

Let us consider an axisymmetric linear elastic material which occupies the domain Ω, with a smooth boundary Γ. We assume that the boundary is divided into three disjoint parts Γ_d, Γ_p and Γ_u, where $\Gamma_d \cup \Gamma_p \cup \Gamma_u = \Gamma$. We also assume that the loadings are axisymmetric.

With no body force, the equilibrium equations in cylindrical coordinates are given by:

$$\frac{\partial \sigma_{rr}}{\partial r} + \frac{\partial \sigma_{rz}}{\partial z} + \frac{\sigma_{rr} - \sigma_{\theta\theta}}{r} = 0$$
$$\frac{\partial \sigma_{rz}}{\partial r} + \frac{\partial \sigma_{zz}}{\partial z} + \frac{\sigma_{rz}}{r} = 0 \tag{1}$$

where r is the radial coordinate, θ is the angular one and z is the longitudinal one.

The Cauchy stress tensor components σ_{ij} are related to the infinitesimal strain tensor components ε_{ij} by the following constitutive equations:

$$\sigma_{ij} = 2\mu\varepsilon_{ij} + \lambda\delta_{ij}\varepsilon_{kk} \tag{2}$$

where λ and μ are the Lamé constants. These are related to Young's modulus E and Poisson's ratio v as:

$$\lambda = \frac{vE}{(1+v)(1-2v)}$$
$$\mu = \frac{E}{2(1+v)}$$

The strain tensor components ε_{ij}, related to the displacement components and to those gradients, are given by:

$$\varepsilon_{rr} = \frac{\partial u_r}{\partial r}, \quad \varepsilon_{\theta\theta} = \frac{u_r}{r}$$
$$\varepsilon_{r\theta} = 0, \quad \varepsilon_{\theta z} = 0 \tag{3}$$
$$2\varepsilon_{rz} = \frac{\partial u_r}{\partial z} + \frac{\partial u_z}{\partial r}, \quad \varepsilon_{zz} = \frac{\partial u_z}{\partial z}$$

By substituting Hooke's law (2) into the governing Eq. (1), the Lamé equations are obtained:

$$(\lambda + 2\mu)\left(\frac{\partial^2 u_r}{\partial r^2} + \frac{1}{r}\frac{\partial u_r}{\partial r} - \frac{u_r}{r^2}\right) + (\lambda + \mu)\frac{\partial^2 u_z}{\partial r \partial z} + \mu\frac{\partial^2 u_r}{\partial z^2} = 0$$

$$(\lambda + 2\mu)\frac{\partial^2 u_z}{\partial z^2} + (\lambda + \mu)\left(\frac{\partial^2 u_r}{\partial r \partial z} + \frac{1}{r}\frac{\partial u_r}{\partial z}\right) + \mu\left(\frac{\partial^2 u_z}{\partial r^2} + \frac{1}{r}\frac{\partial u_z}{\partial r}\right) = 0 \tag{4}$$

These equations can be divided by E and lead to the system of equations $\mathbf{L}(u) = 0$:

$$2(1-v)\left(\frac{\partial^2 u_r}{\partial r^2} + \frac{1}{r}\frac{\partial u_r}{\partial r} - \frac{u_r}{r^2}\right) + \frac{\partial^2 u_z}{\partial r \partial z} + (1-2v)\frac{\partial^2 u_r}{\partial z^2} = 0$$

$$2(1-v)\frac{\partial^2 u_z}{\partial z^2} + \left(\frac{\partial^2 u_r}{\partial r \partial z} + \frac{1}{r}\frac{\partial u_r}{\partial z}\right) + (1-2v)\left(\frac{\partial^2 u_z}{\partial r^2} + \frac{1}{r}\frac{\partial u_z}{\partial r}\right) = 0 \tag{5}$$

At a point $x \in \Gamma$, $n(x)$ is the outward unit normal vector as well as $\mathbf{P}(x)$ is the stress vector whose components are defined by:

$$\mathbf{P_i}(x) = \mathbf{P_i}(u(x)) = \sigma_{ij}(u(x))n_j(x) \quad x \in \Gamma$$

We define the adimensional stress vector by:

$$p_i(x) = \frac{\mathbf{P_i}(x)}{E} \quad x \in \Gamma$$

It is assumed that both the displacement vector $u = (u_r, u_z)$ and the adimensional stress vector $p = (p_r, p_z)$ are given or known on the boundary part Γ_d. It is also assumed that only the adimensional stress vector p is given or known on the boundary part Γ_p but no condition is prescribed on the remaining part Γ_u:

$$u(x) = \phi^d \quad x \in \Gamma_d$$
$$p(x) = \psi^d \quad x \in \Gamma_d \cup \Gamma_p \tag{6}$$

where ϕ^d and ψ^d are prescribed vector functions. The Lamé (or Navier) system (5) and the boundary conditions (6) lead to the formulation of the Cauchy problem in linear elasticity:

$$\begin{cases} \mathbf{L}(u) = 0 & x \in \Omega \\ u(x) = \phi^d & x \in \Gamma_d \\ p(x) = \psi^d & x \in \Gamma_d \cup \Gamma_p \end{cases} \tag{7}$$

This problem is difficult to solve, since it is ill-posed. When it admits a solution, its solution is unique (Yeih et al., 1993), but it is known to be very sensitive (Hadamard, 1923) to small perturbations on boundary conditions (6).

3. The evanescent regularization method

3.1. The iterative algorithm

Let us introduce the space $H(\Omega)$ of solutions of the equilibrium Eq. (5):

$$H(\Omega) = \{v \in H^1(\Omega) \text{ satisfying } \mathbf{L}(v) = 0 \text{ in } \Omega\}$$

Next, let us denote $H(\Gamma)$ the space composed of couples of restrictions on Γ of elements v in $H(\Omega)$ and of their associated stress vector $p(v)$.

$$H(\Gamma) = \{\mathbf{U} = (u,p) \in H^{\frac{1}{2}}(\Gamma) \times H^{-\frac{1}{2}}(\Gamma) / \exists v \in H(\Omega) \text{ such that} : v|_\Gamma = u, p(v)|_\Gamma = p\}$$

An equivalent formulation of problem (7) reads:

$$\begin{cases} \text{Find } \mathbf{U} = (u,p) \in H(\Gamma) \text{ such as :} \\ u = \phi^d \text{ on } \Gamma_d \\ p = \psi^d \text{ on } \Gamma_d \cup \Gamma_p \end{cases} \tag{8}$$

The problem (8) is also ill-posed even if it admits a unique solution. So then an iterative regularizing method is introduced to solve it. Given $c > 0$ and $\mathbf{U^0} \in H(\Gamma)$ the iterative algorithm reads:

$$\left|\begin{array}{l} \text{Find } \mathbf{U^{k+1}} \in H(\Gamma) \text{ such as :} \\ J(\mathbf{U^{k+1}}) \leqslant J(\mathbf{V}) \quad \forall \mathbf{V} \in H(\Gamma) \text{ with} \\ J(\mathbf{V}) = \|v - \phi^d\|^2_{\Gamma_d} + \|p - \psi^d\|^2_{\Gamma_d \cup \Gamma_p} + c\|\mathbf{V} - \mathbf{U^k}\|^2_\Gamma \end{array}\right. \tag{9}$$

where the norms are defined by:

$$\|v\|^2_{\Gamma_d} = \int_{\Gamma_d} v^2 \, ds$$

$$\|p\|^2_{\Gamma_d \cup \Gamma_p} = \int_{\Gamma_d \cup \Gamma_p} p^2 \, ds$$

$$\|\mathbf{V}\|^2_\Gamma = \int_\Gamma v^2 \, ds + \int_\Gamma p^2 \, ds$$

This iterative process is also used in Delvare et al. (2010) to solve the Cauchy problem for the linear elasticity and is a generalization of the inverse technique introduced by Cimetière et al. (2000, 2001) to solve the Cauchy problem for the Laplace equation. It can be considered as an iterative Tikhonov-type method.

In this iterative process, the equilibrium Eq. (5) are taken into account exactly since at each step the search for the optimal element is performed in space $H(\Gamma)$. The functional is composed of three terms which play different roles. The first one (respectively the second one) acts only on Γ_d (respectively only on $\Gamma_d \cup \Gamma_p$). These terms represent the gap between the optimal element and the overspecified boundary data. They relax the overspecified data which can be possibly blurred by measurement noises (relaxation terms). The third term of the functional acts on the whole boundary Γ and not only on the boundary Γ_u where the boundary conditions are to be completed. This term is a regularization term and controls the distance between the new optimal element and the previous one. This term tends to zero as the iterations continue.

So, at each step the optimal element obtained is an exact solution of the equilibrium Eq. (5) and is close to the overspecified data $\mathbf{\Phi^d} = (\phi^d, \psi^d)$.

3.2. Convergence results

The unique optimal element $\mathbf{U^{k+1}} = (u^{k+1}, p^{k+1})$ is characterized, for all $\mathbf{V} = (v, p) \in H(\Gamma)$, by:

$$\langle u^{k+1} - \phi^d, v \rangle_{\Gamma_d} + \langle p^{k+1} - \psi^d, p \rangle_{\Gamma_d \cup \Gamma_p} + c \langle \mathbf{U^{k+1}} - \mathbf{U^k}, \mathbf{V} \rangle_\Gamma = 0 \tag{10}$$

Theorem (*Convergence of the sequence*). *Let* $\mathbf{\Phi^d} = (\phi^d, \psi^d)$ *be compatible data associated with the compatible pair* $\mathbf{U_e} \in H(\Gamma)$. *Then the sequence produced by the iterative scheme* (9) *strongly converges on* Γ_d *and weakly converges to* $\mathbf{U_e}$ *on* Γ, *where* $\mathbf{U_e}$ *is the solution of the problem* (8).

The proof of the theorem is similar to that established for the algorithm introduced in Cimetière et al. (2000) to solve the Cauchy problem associated with the Laplace equation. This proof is valid for all $c > 0$. The c value only influences the convergence rate of the algorithm.

3.3. Properties of the iterative process

Some properties of the functional terms in the minimizing sequence can be easily established without the assumption that the data $\mathbf{\Phi^d} = (\phi^d, \psi^d)$ are compatible:

- The sum of the relaxation terms $\mathbf{S_R}(\mathbf{U^k}) = \|u^k - \phi^d\|^2_{\Gamma_d} + \|p^k - \psi^d\|^2_{\Gamma_d \cup \Gamma_p}$ is monotonically decreasing :

$$\mathbf{S_R}(\mathbf{U^{k+1}}) \leqslant \mathbf{S_R}(\mathbf{U^k}) \tag{11}$$

- The regularization term $J_\Gamma(\mathbf{U^k})$ is monotonically decreasing as soon as $c > 0$:

$$\|\mathbf{U^{k+1}} - \mathbf{U^k}\|^2_\Gamma \leqslant \|\mathbf{U^k} - \mathbf{U^{k-1}}\|^2_\Gamma \tag{12}$$

- The sequence defined by the values of the functional J for each optimal element $\mathbf{U^k}$ is also monotonically decreasing as soon as $c > 0$:

$$J(\mathbf{U^{k+1}}) \leqslant J(\mathbf{U^k}). \tag{13}$$

4. The implementation using the finite element method

4.1. Discrete solutions space

The first issue in this section is to discretize space $H(\Gamma)$. Our main concern has been to make use of any ordinary finite element code. Computations were run using `Cast3M`[1] (CASTEM, 1998) and piecewise linear finite elements, which means a piecewise constant approximation for the stress vector. Let us now discretize the domain Ω, h being the discretization parameter standing for the element size, leading to n nodes and n elements on the boundary, and m nodes inside the domain. Let V_h be the space of continuous piecewise linear functions with respect to the mesh, and let us define $V_h(\Gamma)$ and $W_h(\Gamma)$ as the space of continuous piecewise linear functions and the space of piecewise constant functions on the boundary. Traces of functions belonging to $V_h(\Omega)$ span the space $V_h(\Gamma)$, whereas the associated stress vectors belong to the space $W_h(\Gamma)$ of piecewise constant functions. Defining U and P as the $2n$ vectors standing respectively for the $2n$ nodal values of u and the $2n$ discrete values of p on the boundary, and U^* the $2m$-vector of internal nodal values of u, the discrete equilibrium equations read as:

$$\begin{bmatrix} A_{ii} & A_{ei}^T \\ A_{ei} & A_{ee} \end{bmatrix} \begin{pmatrix} U^* \\ U \end{pmatrix} = \begin{pmatrix} 0 \\ -BP \end{pmatrix} \tag{14}$$

A_{ii} is the stiffness matrix corresponding to the Dirichlet problem and is thus invertible. Expressing the internal unknowns U^* in terms of the boundary ones U, i.e performing a condensation, Eq. (14) reduces to:

$$\left(A_{ee} - A_{ei} A_{ii}^{-1} A_{ei}^T \right) U + BP = 0 \tag{15}$$

The matrix form of (15) reads:

$$[A \quad B] \begin{pmatrix} U \\ P \end{pmatrix} = 0 \tag{16}$$

The finite element method leads to the definition of the following discrete compatible pairs space which reads:

$$H_h(\Gamma) = \left\{ \begin{array}{l} (U, P) \in \mathbb{R}^{2n} \times \mathbb{R}^{2n} \text{ such that} \\ E_h(U, P) = AU + BP = 0 \end{array} \right\} \tag{17}$$

where E_h denotes a linear operator mapping $\mathbb{R}^{2n} \times \mathbb{R}^{2n}$ onto $\mathbb{R}^{2n}$.

4.2. Discretization of the (k + 1)th iteration

Given now $c > 0$ and $(U^k, P^k) \in H_h(\Gamma)$, iteration $(k + 1)$ of the discretized iterative algorithm reads as follows:

$$\left| \begin{array}{l} \text{Find } (U^{k+1}, P^{k+1}) \in \mathbb{R}^{2n} \times \mathbb{R}^{2n} \text{ such that :} \\ J(U^{k+1}, P^{k+1}) \leqslant J(V, Q) \forall (V, Q) \in \mathbb{R}^{2n} \times \mathbb{R}^{2n} \\ \text{under the } 2n \text{ scalar equality constraints } E_h(V, Q) = 0 \end{array} \right. \quad (18)$$

Problem (18) is a minimization problem in $R^{2n} \times R^{2n}$ under the $2n$ equality constraints expressed by (16). Its solution is given by:

$$\left| \begin{array}{l} \text{Initializing with } (U^0 = 0, P^0 = 0) \\ \text{Find } (U^{k+1}, P^{k+1}, \lambda^{k+1}) \in \mathbb{R}^{2n} \times \mathbb{R}^{2n} \times \mathbb{R}^{2n} \text{ such that :} \\ \nabla J(U^{k+1}, P^{k+1}) + (\lambda^{k+1})^T \nabla E_h(U^{k+1}, P^{k+1}) = 0 \\ E_h(U^{k+1}, P^{k+1}) = 0 \end{array} \right. \quad (19)$$

where λ^{k+1} is a $2n$-vector of Lagrange multipliers introduced to take the equality constraints (16) into account. Each iteration in the iterative algorithm needs to solve a system of $6n$ linear equations with $6n$ unknowns. The matrices of this linear system is independent of the iterations and needs to be computed only once. For this reason, a direct algorithm (the Crout factorization) has been preferred to iterative methods. The factorization, which is obtained at the first step, is also used at each following step.

In the case of compatible data, the proof of the convergence of the discrete algorithm is similar to that established for the corresponding algorithm used to solve the Cauchy problem for the Laplace equation (Cimetière et al., 2000). This proof is valid for all $c > 0$ and the c value only influences the convergence rate of the algorithm.

4.3. Numerical procedure

The procedure used during the numerical simulations is as follows:

(i) The meshing of the boundary is made using SEG2 elements. The SEG2 element is a finite element with two nodes which leads to a linear interpolation of the displacements. This induces a piecewise constant interpolation of the stress vector components.

(ii) The user specifies the meshing of the boundary specifying the number and the distribution of the finite elements on each part of the boundary.

(iii) The mesh of the entire domain is generated automatically by a routine included in the Cast3m software. This mesh is constituted by 4-node quadrilaterals.

(iv) The computation and the assembly of the stiffness matrix corresponding to the domain is performed thanks to the standard routines of the Cast3m software.

(v) This software generates a superelement based on the boundary and computes the corresponding stiffness matrix. This leads to the condensed stiffness matrix A.

(vi) The stiffness matrix A is then used by the specific code that implements the inverse method introduced.

Note that all numerical computations have been performed on a machine with a 2.20 GHz Intel® Core™ 2 Duo processor T7500.

The following control quantities are used to estimate the accuracy of the method:

– the $L^2(\Gamma)$ relative error made on u:

$$u_{error} = \sqrt{\frac{\int_{\Gamma} (u - u^{an})^2 \, ds}{\int_{\Gamma} (u^{an})^2 \, ds}}$$

– the $L^2(\Gamma)$ relative error made on p:

$$p_{error} = \sqrt{\frac{\int_{\Gamma} (p - p^{an})^2 \, ds}{\int_{\Gamma} (p^{an})^2 \, ds}}$$

where u^{an} and p^{an} denote the analytical solution.

5. Numerical results using analytical reference solutions

The purpose of this section is to present numerical results obtained with the method introduced. Firstly, different cases are considered for which an analytical solution is known.

5.1. Examples

A two-dimensional isotropic linear elastic medium in an axisymmetric stress state characterized by the material constants $E = 200$ GPa and $v = 0.34$ corresponding to a steel is studied.

The domain Ω (Fig. 1) is defined by:

$$\Omega = \left\{ (r,z) / R_1 < r < R_2, \quad -\frac{h}{2} < z < \frac{h}{2} \right\}$$
with $R_1 = 0.01$ m, $R_2 = 0.014$ m and $h = 0.04$ m.

The boundary part Γ_d is defined by:

$$\Gamma_d = \{ (r,z) \in \Gamma / r = R_2 \}$$

Γ_d is discretized using 160 finite elements SEG2. All finite elements have the same length and the nodes are uniformly distributed. The boundary part Γ_u is defined by:

$$\Gamma_u = \{ (r,z) \in \Gamma / r = R_1 \}$$

and discretized using a regular mesh with 160 finite elements SEG2. The boundary part Γ_p is defined by:

$$\Gamma_p = \left\{ (r,z) \in \Gamma / z = \pm \frac{h}{2} \right\}$$

and each side is discretized using a regular mesh with 20 finite elements SEG2. It is used to find the displacement and the stress
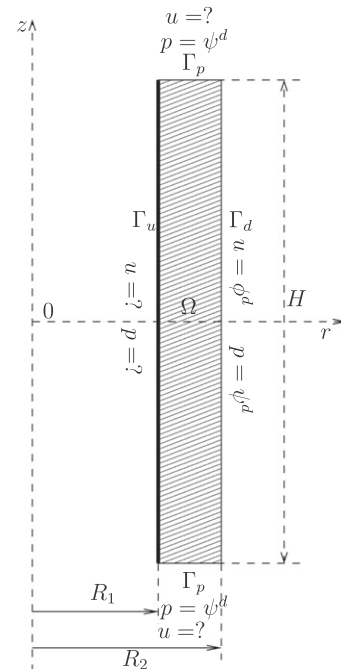

Fig. 1. The domain Ω, the boundary part Γ_d, the boundary part Γ_p, the boundary part Γ_u and the specified boundary conditions for the inverse problems investigated in Examples 1 and 2.

vectors on Γ_u, from the knowledge of the displacement on Γ_d and the stress vectors on $\Gamma_d \cup \Gamma_p$.

5.1.1. Example 1

The data are built using the following analytical solution for the displacements:

$$u_r(r,z) = \frac{KR_1(1-v)r}{E\Delta} + \frac{KR_1R_2^2(1+v)}{rE\Delta} \tag{20}$$

$$u_z(r,z) = \frac{2vKR_1(H-z)}{E\Delta} \tag{21}$$

where $\Delta = \frac{R_2^2 - R_1^2}{R_1}$ and with $K = 0.01\,E$. The corresponding components of the stress tensor are:

$$\sigma_{rr}(r,z) = K\frac{R_1}{\Delta}\left(1 - \frac{R_2^2}{r^2}\right), \tag{22}$$

$$\sigma_{\theta\theta}(r,z) = K\frac{R_1}{\Delta}\left(1 + \frac{R_2^2}{r^2}\right), \tag{23}$$

$$\sigma_{rz}(r,z) = 0, \tag{24}$$

$$\sigma_{zz}(r,z) = 0, \tag{25}$$

which correspond to a constant internal radial stress $\mathbf{P_r}(z) = K$ (or its dimensionless expression $p_r(z) = \frac{K}{E}$) on Γ_u and a free-force boundary $\Gamma_d \cup \Gamma_p$.

5.1.2. Example 2

The data are built using the following analytical solution for the displacements:

$$u_r(r,z) = \frac{2K(1+v)}{E\Delta}\left(\begin{array}{c} A_1 z^2\left(r + \frac{R_2^2}{r}\right) - A_2 r^3 \\ + A_3 R_2^2 r \ln\frac{r}{R_2} + A_4 R_2^2 r \end{array}\right) \tag{26}$$

$$u_z(r,z) = \frac{2K(1+v)}{E\Delta}\left(\begin{array}{c} z\left(B_1 r^2 - B_2 R_2^2 \ln\frac{r}{R_2} + B_3 R_2^2\right) \\ - B_4 z^3 \end{array}\right) \tag{27}$$

where

$$\Delta = \frac{R_2^2 - R_1^2}{R_1}, \quad A_1 = \frac{1}{4}, \quad A_2 = \frac{1}{16}, \quad A_3 = \frac{1+v}{4(1-v)},$$

$$A_4 = \frac{2v^2 - 2v + 1}{(1-v)(1-2v)}A_3 - \frac{3+v}{16(1-v)}, \quad B_1 = \frac{1}{4}, \quad B_2 = \frac{3}{2},$$

$$B_3 = \frac{3(1-2v)}{16v} - \frac{1-v}{v}A_3 - \frac{1}{v}A_4, \quad B_4 = \frac{1}{6}$$

and with $K = 220\,\text{GPa m}^{-1}$. The corresponding components of the stress tensor are:

$$\sigma_{rr}(r,z) = \frac{K}{\Delta}\left(\begin{array}{c} \frac{z^2}{2}\left(1 - \frac{R_2^2}{r^2}\right) + \frac{3}{8}\left(R_2^2 - r^2\right) \\ + \frac{1-3v}{2(1-v)}R_2^2 \ln\left(\frac{r}{R_2}\right) \end{array}\right) \tag{28}$$

$$\sigma_{rz}(r,z) = \frac{Kz}{\Delta}\left(r - \frac{R_2^2}{r}\right) \tag{29}$$

$$\sigma_{zz}(r,z) = \frac{K}{\Delta}\left(\frac{R_2^2 - r^2}{2} - \frac{3-v}{1-v}R_2^2 \ln\frac{r}{R_2} - z^2\right) \tag{30}$$

which correspond to the following stress vector $\mathbf{P}(z)$ on Γ_u:

$$\mathbf{P_r}(z) = -\frac{K}{\Delta}\left(\begin{array}{c} \frac{z^2}{2}\left(1 - \frac{R_2^2}{R_1^2}\right) + \frac{3}{8}\left(R_2^2 - R_1^2\right) \\ + \frac{3v-1}{2(1-v)}R_2^2 \ln\left(\frac{R_2}{R_1}\right) \end{array}\right)$$

$$\mathbf{P_z}(z) = Kz$$

and to its dimensionless expression $p(z) = \frac{\mathbf{P}(z)}{E}$.

5.2. Stopping criterion and influence of parameter c

In a first step, a reliable stopping criterion is needed to stop the iterative process. As in Delvare et al. (2010), the determination of the iteration to stop the iterative process is made using the quantity $J(\mathbf{U^{k+1}})$ where $\mathbf{U^{k+1}}$ is the optimal element obtained at the $(k+1)$th step. The evolution of J versus the number of iterations k follows an L-curve (Hansen, 1992). As expected from relation (13), the control quantity J decreases and then becomes almost constant. So the iterative process is stopped when J becomes almost constant. This stopping criterion is blind because when calculating the quantity J it does not need to know the analytical solution. Indeed, it only needs to know two successive optimal elements, the displacements data on Γ_d and the pressure data on $\Gamma_d \cup \Gamma_p$. As expected from relation (12), we may also notice that J_Γ (the regularization term) decreases as the iterations continue. This term becomes negligible compared to the sum $\mathbf{S_R}$ of the relaxation terms and tends to zero. This proves that the algorithm converges. As expected from relation (11), the sum $\mathbf{S_R}$ decreases during the iterative process. After convergence, this sum remains constant and corresponds to the approximation error of the finite element method when the data are not noisy. When the displacements data ϕ^d are noisy, after convergence, the residual value of the sum $\mathbf{S_R}$ corresponds to the distance on the supports of data between the deblurred reconstructions and the noisy data.

It is also necessary to look at the influence of parameter c which defines the relative weight of the regularization term compared to the relaxation terms. Different values of the parameter c are tested. Table 1 lists the results obtained for each value of parameter c by specifying the number of iterations necessary to achieve convergence, the u_{error}, the p_{error} and the CPU time. The errors on u and p are quite identical for each value of the parameter c. This confirms that the algorithm converges to the same solution whatever the value of c. However, the choice of the parameter c affects the number k of iterations needed to obtain convergence. The number of iterations necessary to achieve convergence evolves linearly with c. From the evolution of the CPU time with c (or with the number of iterations k) it can be deduced that the CPU time taken by each iteration for $k > 1$ is roughly 1.15×10^{-2} s. This CPU time is less than the CPU time taken to achieve both the preliminary computations and the first iteration (roughly 4.23 s). For a small value of c, the convergence only takes a few iterations, however the p_{error} increases a little. This may be explained by the fact that the regularization term becomes too weak and induces some instabilities on the reconstructions. Moreover, it is preferable to have a greater value of the parameter c which induces little additional CPU time in order to have more accurate reconstructions. Subsequently, the value of c and the number of iterations required to achieve convergence will be no longer specified.

It can also be observed that the errors in the numerical stresses obtained (p_{error}) using the iterative method are larger than those corresponding to the reconstructed displacements (u_{error}). This last remark is also valid for all the following numerical examples which will be analyzed.

Table 1
Influence of c on the number of iterations k to achieve convergence – influence of c on the u_{error} and on the p_{error}.

c	k	u_{error} (%)	p_{error} (%)	CPU time (s)
1e−4	182,404	0.0138653	0.543446	2103.65
1e−5	18,242	0.0138653	0.543447	214.10
1e−6	1825	0.0138649	0.543439	25.21
1e−7	184	0.0138617	0.543480	6.34
1e−8	20	0.0138480	0.544349	4.45
1e−9	3	0.0140402	0.549715	4.23

5.3. Reconstruction on Γ_u with noisy displacement data ϕ^d

It is necessary to see how the reconstructions are influenced when both components of the displacement data ϕ^d are noisy. The noisy displacement data ϕ^d are generated by:

$$\phi^d = \phi^d_{an} + \delta\eta\phi^d_{max} \qquad (31)$$

where $-1 \leqslant \eta \leqslant 1$ is a random value, δ is the noise level in % and ϕ^d_{max} is the maximal value of the data of Γ_d.

Fig. 2 (respectively, Fig. 3) shows the reconstructions on Γ_u of the u_r-component (respectively, u_z-component) of the displacement obtained with different noise levels ($\delta = 1\%$ and $\delta = 5\%$) for Example 1. On the same figures, these reconstructions are compared with the reconstruction obtained with no noisy data. Fig. 4 (respectively, Fig. 5) gives the corresponding reconstructions of the p_r-component (respectively, p_z-component) of the stress vector. Figs. 6–9 give the corresponding reconstructions for Example 2.

All the reconstructions of the components of the displacement obtained can be seen to be very accurate. It can also be observed that the reconstructions of the components of the stress vector obtained using the iterative method are less accurate than those corresponding to the displacement vector.

5.4. Reconstruction on Γ_d : Deblurring the noisy displacement data ϕ^d

The functional is composed of terms which play different roles. As in most inverse methods, there is a regularization term which tends to zero as the iterations continue. But, in the present case, there are also relaxation terms that allow data blurred by noise to be taken into account. We therefore seek a solution which is close to the data but not a solution that exactly fits the data. The algorithm then recomputes, at each step, a solution on the whole boundary.

Fig. 10 (respectively, Fig. 11) gives the reconstruction of the u_r-component of the displacement (respectively, the u_z-component) on Γ_d and the noisy data ϕ^d used ($\delta = 5\%$) for Example 1. Figs. 12 and 13 give the corresponding reconstructions for Example 2. It can be noted that all these reconstructions correspond to the ana-
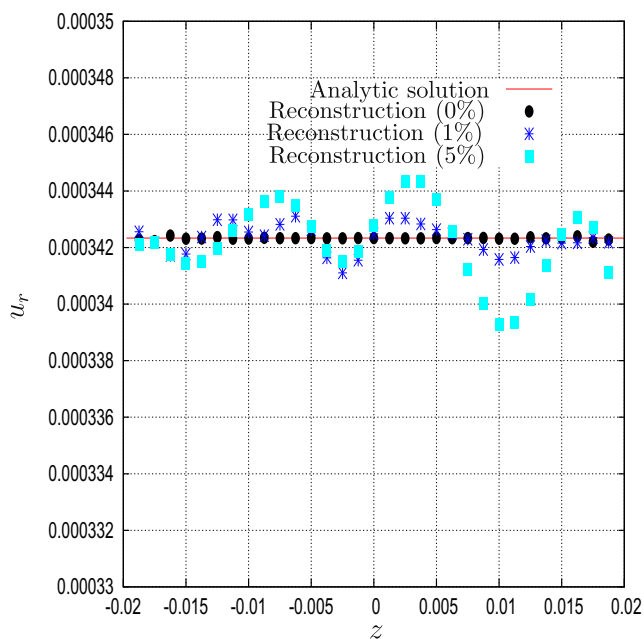

Fig. 3. The analytical solution and the numerical reconstructions of the u_z-component of the displacement obtained on Γ_u, for $\delta = 0\%$, $\delta = 1\%$ and $\delta = 5\%$, for the Cauchy problem considered in Example 1.
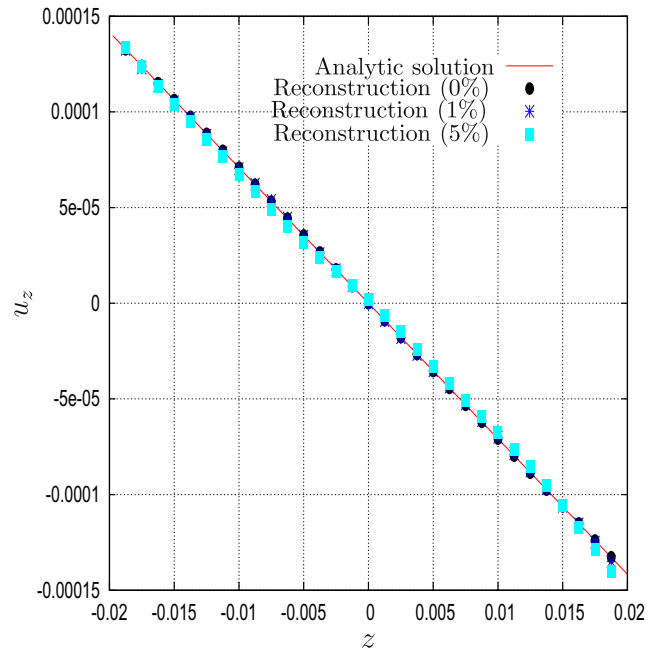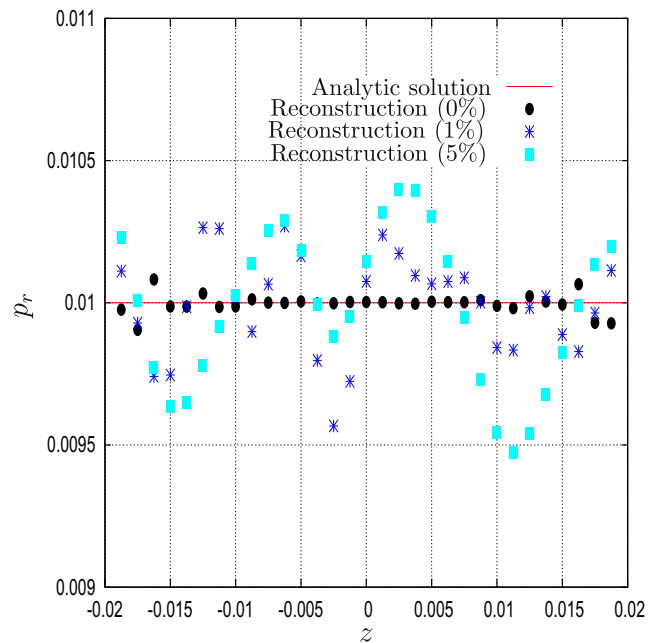

Fig. 4. The analytical solution and the numerical reconstructions of the radial stress p_r obtained on Γ_u, for $\delta = 0\%$, $\delta = 1\%$ and $\delta = 5\%$, for the Cauchy problem considered in Example 1.

lytical solution and that the noise in the data has been deleted by the algorithm.

Fig. 14 represents, for Example 1, the evolution of the functional terms S_R, J_Γ and J versus the number of iterations k when the data ϕ^d is noisy ($\delta = 5\%$). After convergence, the regularization term J_Γ is negligible and the residual term J is equal to the sum of the relaxation terms. This residual term corresponds to the distance on Γ_d between the deblurred reconstruction and the noisy data. It can also be noted that the relations (11)–(13) are also verified when the data ϕ^d is noisy. This is not surprising because the inequalities
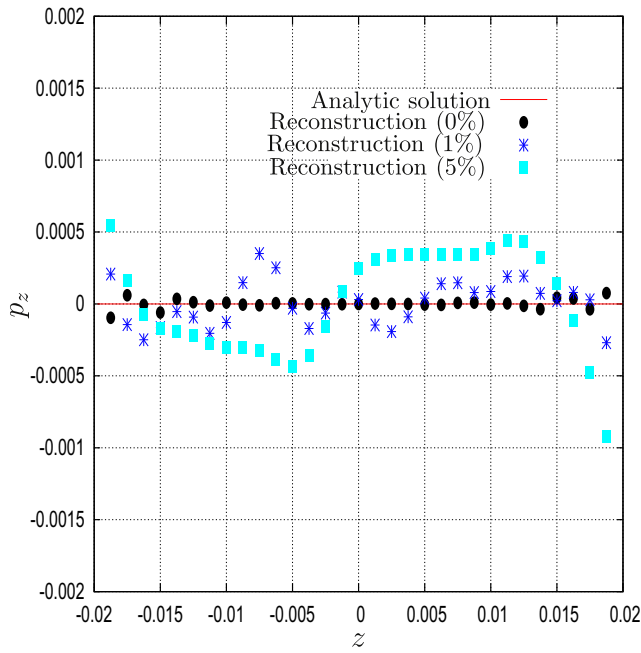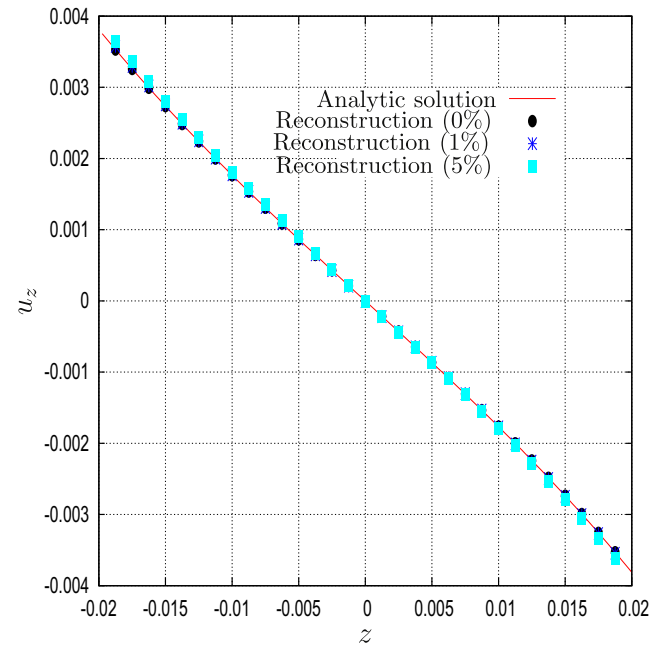

Fig. 2. The analytical solution and the numerical reconstructions of the u_r-component of the displacement obtained on Γ_u, for $\delta = 0\%$, $\delta = 1\%$ and $\delta = 5\%$, for the Cauchy problem considered in Example 1.
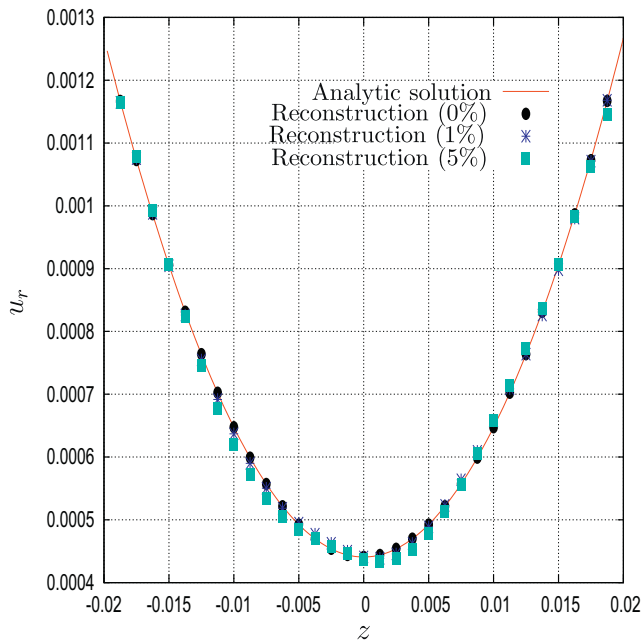
Fig. 5. The analytical solution and the numerical reconstructions of the axial stress p_z obtained on Γ_u, for $\delta = 0\%$, $\delta = 1\%$ and $\delta = 5\%$, for the Cauchy problem considered in Example 1.

Fig. 7. The analytical solution and the numerical reconstructions of the u_z-component of the displacement obtained on Γ_u, for $\delta = 0\%$, $\delta = 1\%$ and $\delta = 5\%$, for the Cauchy problem considered in Example 2.

Fig. 6. The analytical solution and the numerical reconstructions of the u_r-component of the displacement obtained on Γ_u, for $\delta = 0\%$, $\delta = 1\%$ and $\delta = 5\%$, for the Cauchy problem considered in Example 2.

Fig. 8. The analytical solution and the numerical reconstructions of the radial stress p_r obtained on Γ_u, for $\delta = 0\%$, $\delta = 1\%$ and $\delta = 5\%$, for the Cauchy problem considered in Example 2.

were established without any assumptions on the data (for instance that $\boldsymbol{\Phi^d}$ is compatible).

5.5. Behaviour with respect to the mesh refinement

It is necessary to see how the reconstructions are influenced when the mesh refinement of the boundary Γ increases. In this section, the boundary part Γ_d is discretized using $8N$ finite elements SEG2 where all finite elements have the same length and the nodes are uniformly distributed. The boundary part Γ_u is dis-
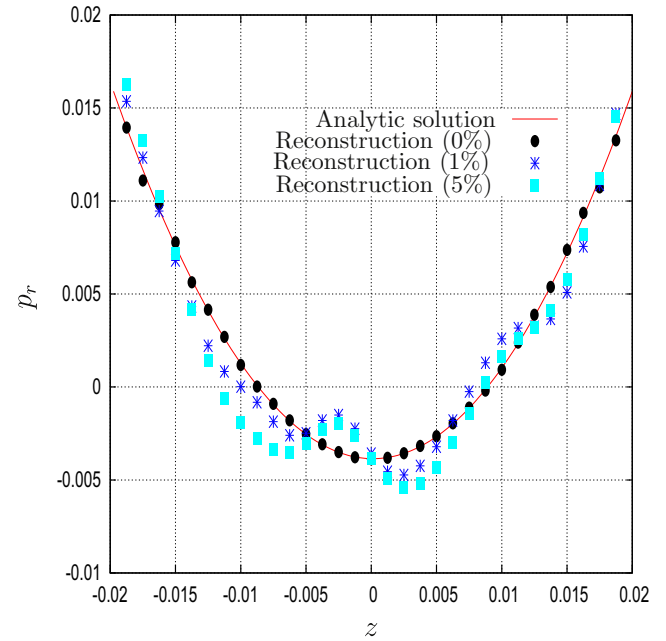
cretized using a regular mesh with $8N$ finite elements SEG2 and both sides of the boundary part Γ_p are discretized using a regular mesh with N finite elements SEG2. The level of noise δ added into the boundary displacement data ϕ^d is fixed to 5%.

Fig. 15 shows the reconstructions on Γ_u of the u_r-component of the displacement u obtained with $N = 5$, $N = 10$ and $N = 20$. Fig. 16 gives the corresponding reconstructions of the p_r-component of the stress vector. These figures confirm that the inverse method is stable with respect to the mesh refinement. Similar results,
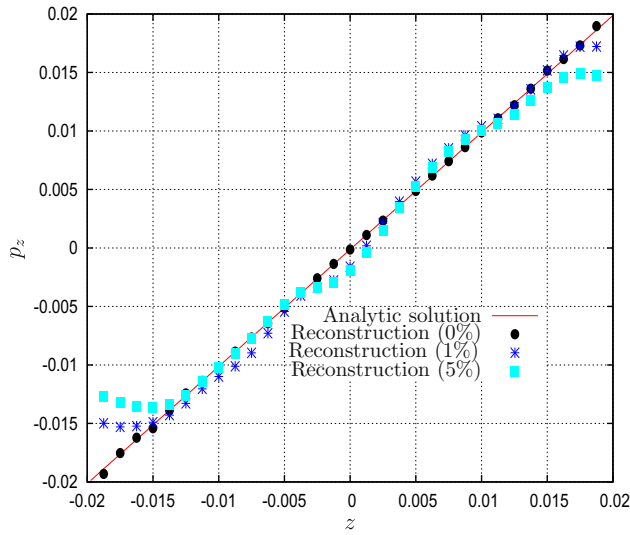
Fig. 9. The analytical solution and the numerical reconstructions of the axial stress p_z obtained on Γ_u, for $\delta = 0\%$, $\delta = 1\%$ and $\delta = 5\%$, for the Cauchy problem considered in Example 2.
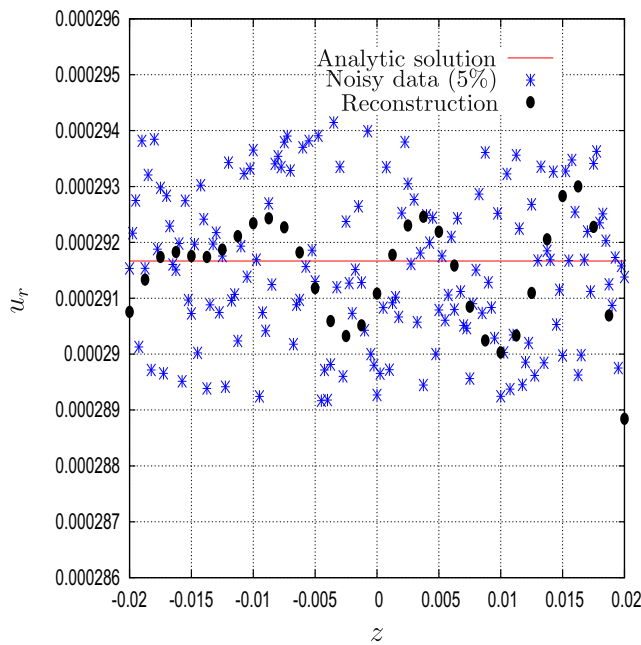

Fig. 11. The analytical solution, the noisy data used ($\delta = 5\%$) and the numerical reconstruction of the u_z-component of the displacement obtained on Γ_d, for the Cauchy problem considered in Example 1.

Fig. 10. The analytical solution, the noisy data used ($\delta = 5\%$) and the numerical reconstruction of the u_r-component of the displacement obtained on Γ_d, for the Cauchy problem considered in Example 1.

Fig. 12. The analytical solution, the noisy data used ($\delta = 5\%$) and the numerical reconstruction of the u_r-component of the displacement obtained on Γ_d, for the Cauchy problem considered in Example 2.

which are not presented here, are obtained for the u_z-component of the displacement and for the p_z-component of the stress vector.

5.6. Behaviour with respect to the extension of the supports of data

In this section, we look at the influence of the type of prescribed data on the numerical solution. We investigate the numerically retrieved solutions corresponding to the following three cases associated with the given data:

Case 1: $u = \phi^d \in \Gamma_d$ and $p = \psi^d \in \Gamma_d \cup \Gamma_p$.
Case 2: $u = \phi^d \in \Gamma_d \cup \Gamma_p$ and $p = \psi^d \in \Gamma_d$.
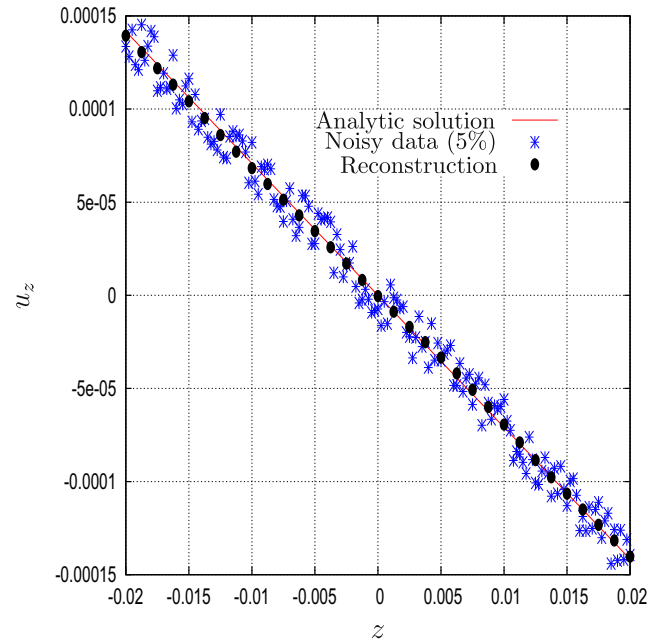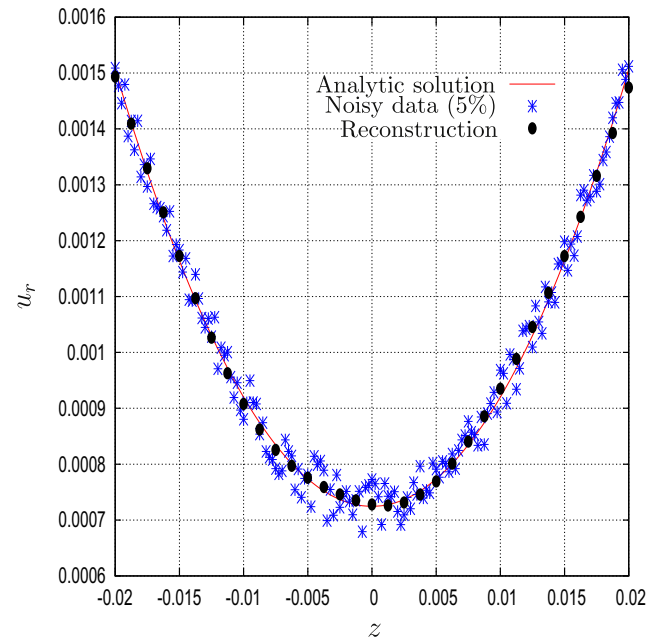Case 3: $u = \phi^d \in \Gamma_d \cup \Gamma_p$ and $p = \psi^d \in \Gamma_d \cup \Gamma_p$.

For the three cases, the same mesh is used and the level of noise δ added into the boundary displacement data ϕ^d is fixed to 5%. The boundary part Γ_d is discretized using 160 finite elements with a regular mesh. The boundary part Γ_u is discretized using a regular mesh with 160 finite elements and both sides of the boundary part Γ_p are discretized using a regular mesh with 20 finite elements.

Fig. 17 shows the reconstructions on Γ_u of the u_r-component of the displacement u obtained for the three cases. Fig. 18 gives the corresponding reconstructions of the p_r-component of the stress vector. These figures confirm that the inverse method is accurate in each case but the reconstructions are more accurate when the
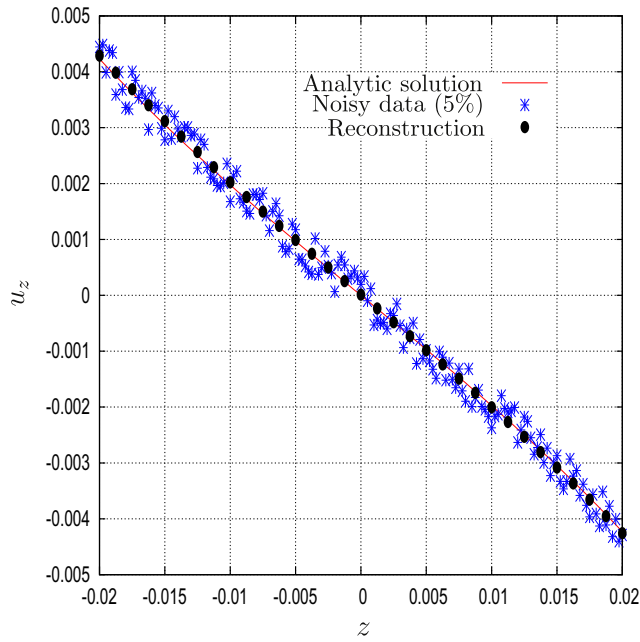
Fig. 13. The analytical solution, the noisy data used ($\delta = 5\%$) and the numerical reconstruction of the u_z-component of the displacement obtained on Γ_d, for the Cauchy problem considered in Example 2.
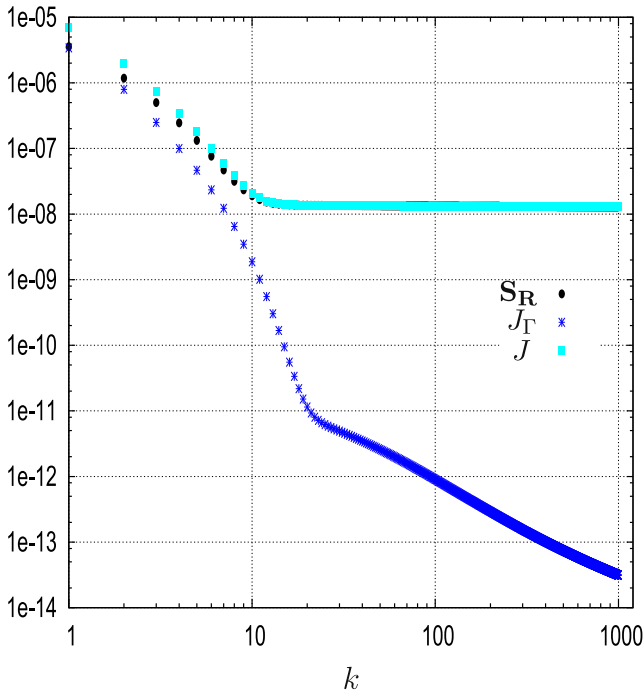

Fig. 15. The analytical solution and the numerical reconstructions of the u_r-component of the displacement obtained on Γ_u, for $\delta = 5\%$ and different mesh refinements $N = 5$, $N = 10$ and $N = 20$, for the Cauchy problem considered in Example 1.

Fig. 14. Evolution of the terms of the functional versus the number of iterations k for $\delta = 5\%$ and for the Cauchy problem considered in Example 1.

Fig. 16. The analytical solution and the numerical reconstructions of the radial stress p_r obtained on Γ_u, for $\delta = 5\%$ and different mesh refinements $N = 5$, $N = 10$ and $N = 20$, for the Cauchy problem considered in Example 1.

extension of the supports of data is greater (case 3). Similar results, which are not presented here, are obtained for the u_z-component of the displacement and for the p_z-component of the stress vector.

6. Application of the method to the identification of a friction coefficient

6.1. Scope of the study

Some materials, like concretes, rocks or geomaterials, have a material behavior which depends on the first invariant
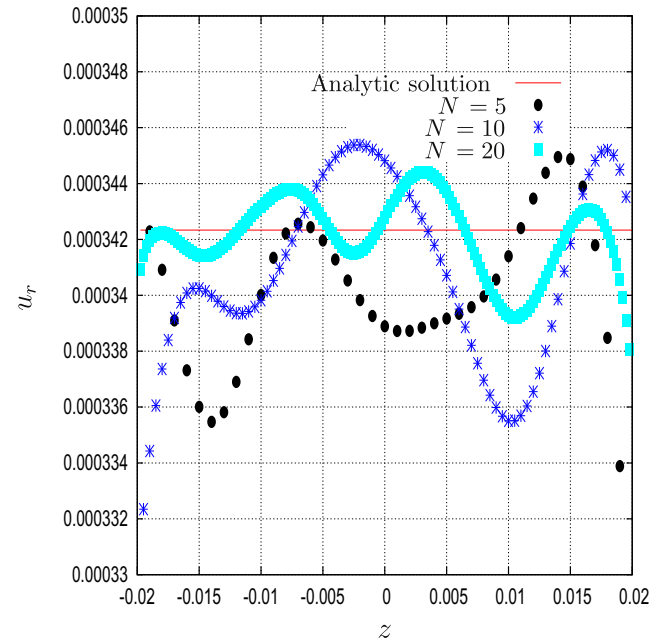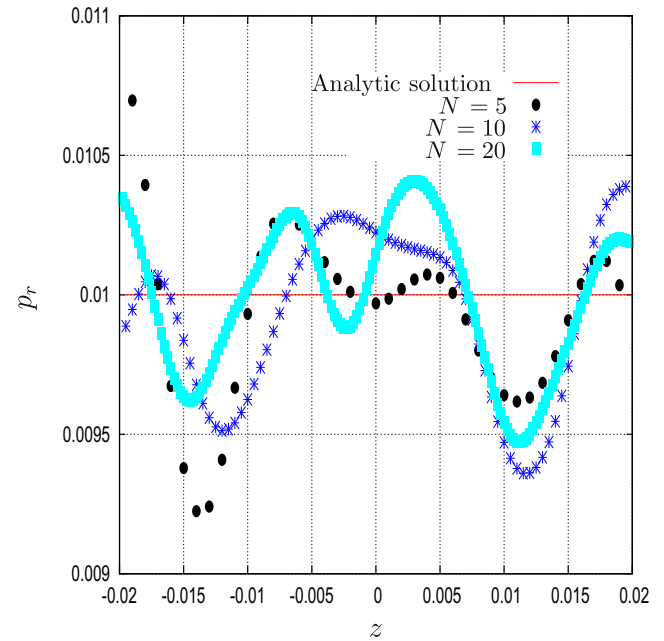
$I_1 = \frac{1}{3}\mathrm{Trace}\,\underline{\sigma}$ of the stress tensor. In order to determine this dependence, some experimental devices have been developed to perform triaxial tests in quasi-static or dynamic situations. For one of them, the confining stress is obtained by placing the specimen in a metallic sleeve to achieve passive confinement (Fig. 19a). The compressive stress is applied directly on the specimen. The metallic ring is then subjected to internal pressure due to the lateral expansion of the specimen. This technique allows a higher level of I_1 to be obtained and has been used in quasi-static (Forquin

et al., 2007) or dynamic situations (Bailly et al., 2011; Gary et al., 1998; Forquin et al., 2008).

Assuming a frictionless contact between the specimen and the metallic ring and assuming an elastic or a perfect elastoplastic behavior of the ring, the analytical solution of a hollow cylinder submitted to inner radial pressure, enables the radial stress on the inner surface of the ring to be deduced from the deformation recorded by a unique gauge glued at the outer surface (Bailly et al., 2011).

The objective is to prove that the inverse data completion method proposed could be very useful when friction at the interface between the specimen and an elastic ring occurs. The specimen could then be replaced by the unknown loading it applies to the elastic ring (Fig. 19b). This unknown loading must be identified by an inverse technique, leading to a Cauchy problem (7).

6.2. Determination of the numerical reference solution using FEM

In order to validate the procedure, we will use a numerical reference solution to a similar problem. The response of the elastic ring made of steel (Young's modulus $E = 220\,\text{GPa}$ and $v = 0.34$) is studied. The loading is defined by the following dimensionless stress distributions along Γ_u:

$$p_r(z) = \begin{cases} a\exp\left(-\beta\left(z+\frac{h}{4}\right)\right) & -\frac{h}{2} \leqslant z \leqslant -\frac{h}{4} \\ b\cosh(\alpha z) & -\frac{h}{4} \leqslant z \leqslant \frac{h}{4} \\ a\exp\left(\beta\left(z-\frac{h}{4}\right)\right) & \frac{h}{4} \leqslant z \leqslant \frac{h}{2} \end{cases} \tag{32}$$

$$p_z(z) = \begin{cases} fp_r(z) & -\frac{h}{2} \leqslant z \leqslant -\frac{h}{4} \\ c\sinh(\alpha z) & -\frac{h}{4} \leqslant z \leqslant \frac{h}{4} \\ -fp_r(z) & \frac{h}{4} \leqslant z \leqslant \frac{h}{2} \end{cases} \tag{33}$$

where $f = 0.13$, $a = 1.031$, $b = 0.963$, $c = -0.350$, $\alpha = 37.435\,\text{m}^{-1}$ and $\beta = 13.394\,\text{m}^{-1}$. The values of these parameters are fixed assuming:

– The contact law is governed by a Coulomb-type criterion:

$$|p_z(z)| \leqslant f|p_r(z)| \tag{34}$$
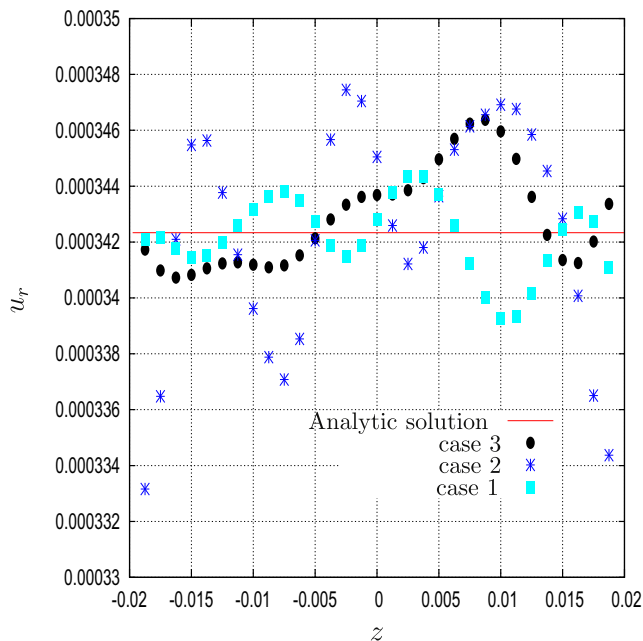
where f is the friction parameter.

Fig. 17. The analytical solution and the numerical reconstructions of the u_r-component of the displacement obtained on Γ_u, for $\delta = 5\%$ and different types of prescribed data, for the Cauchy problem considered in Example 1.
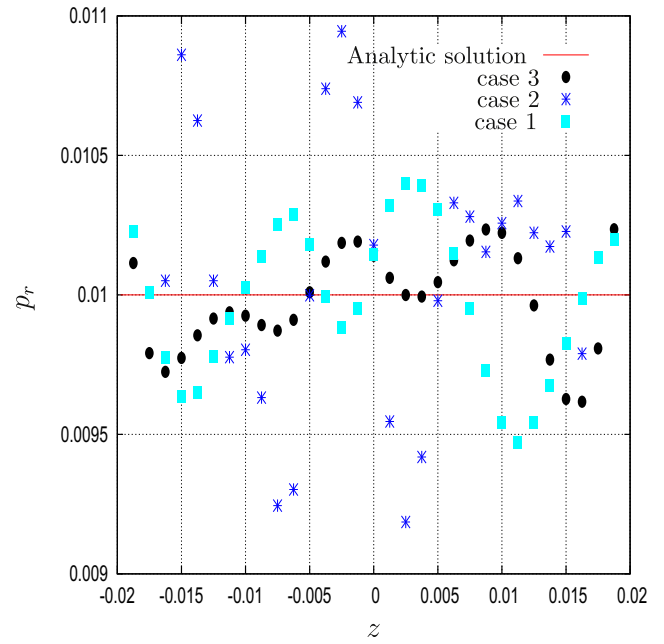
Fig. 18. The analytical solution and the numerical reconstructions of the radial stress p_r obtained on Γ_u, for $\delta = 5\%$ and different types of prescribed data, for the Cauchy problem considered in Example 1.
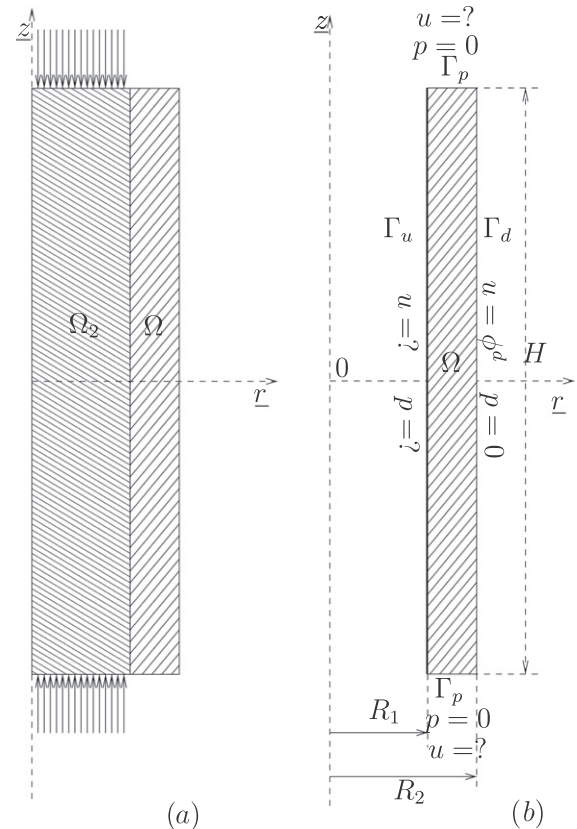
Fig. 19. (a) Schematic representation of the confining test and (b) the domain Ω, the boundary part Γ_d, the boundary part Γ_p, the boundary part Γ_u and the specified boundary conditions for the inverse problems investigated in Example 3.

– The distribution of the radial stress p_r and of the axial stress p_z are continuous along Γ_u.
– The zone defined by $-\frac{h}{4} \leqslant z \leqslant \frac{h}{4}$ is an adherence zone.

– The zones defined by $-\frac{h}{2} \leqslant z \leqslant -\frac{h}{4}$ and $\frac{h}{4} \leqslant z \leqslant \frac{h}{2}$ are sliding zones.

The boundary part $\Gamma_d \cup \Gamma_p$ is also assumed to be a free-force boundary. Then, a standard direct finite element simulation is performed determining a numerical reference solution. The FEM computing code used is always Cast3m. The boundary and the domain meshes used are the same as those used in Section 5. Subsequently, a restriction of this numerical reference solution will be used to determine the input data for the Cauchy problem (7).

6.3. Example 3

Given that $\Gamma_d \cup \Gamma_p$ is a free-force boundary, ψ^d is zero. For this example, only the u_r-component of the displacement is noisy. This noisy data u_r^d is generated by:

$$u_r^d = u_r^{ref} + \eta\delta \tag{35}$$

where $-1 \leqslant \eta \leqslant 1$ is a random value, δ is the noise level due to uncertainties on the radial displacement measurements and u_r^{ref} is the restriction to Γ_d of the radial displacement obtained by direct simulation.

6.4. Reconstructions on Γ_u

Fig. 20 (respectively, Fig. 21) shows the reconstructions on Γ_u of the u_r-component (respectively, u_z-component) of the displacement obtained with different uncertainty levels ($\delta = 5 \times 10^{-5}$, $\delta = 1 \times 10^{-4}$ and $\delta = 5 \times 10^{-4}$). On the same figures, these reconstructions are compared on one side to the reconstruction obtained with no noisy data and on the other side to the reference solution obtained by the direct simulations. Each reconstruction of the components of the displacement can be seen to be very accurate. Fig. 22 (respectively Fig. 23) gives the corresponding reconstructions of the component p_r (respectively, p_z) of the stress vector. The reconstruction of the components of the load is less accurate
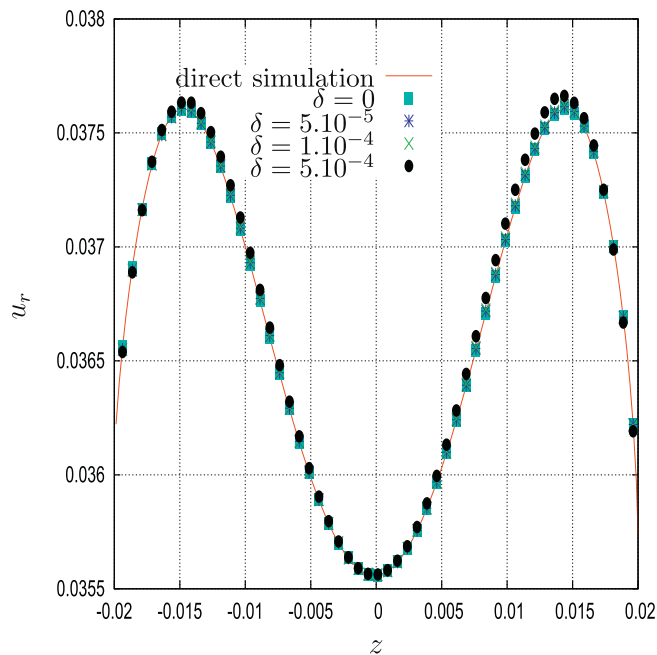

Fig. 20. The numerical reference solution and the numerical reconstructions of the u_r-component of the displacement obtained on Γ_u, for $\delta = 5 \times 10^{-5}$, $\delta = 1.10^{-4}$ and $\delta = 5 \times 10^{-4}$, for the Cauchy problem considered in Example 3.
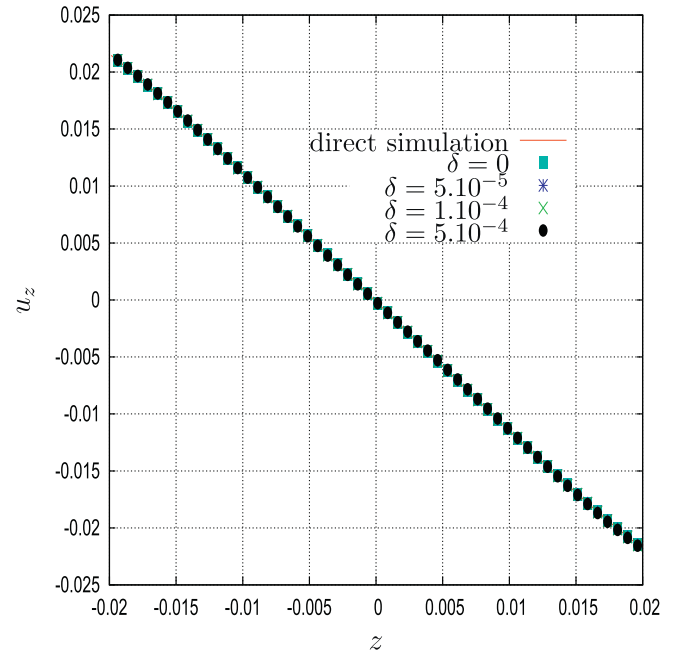

Fig. 21. The numerical reference solution and the numerical reconstructions of the u_z-component of the displacement obtained on Γ_u, for $\delta = 5 \times 10^{-5}$, $\delta = 1 \times 10^{-4}$ and $\delta = 5 \times 10^{-4}$, for the Cauchy problem considered in Example 3.

Fig. 22. The reference value and the numerical reconstructions of the radial stress p_r obtained on Γ_u, for $\delta = 5 \times 10^{-5}$, $\delta = 1 \times 10^{-4}$ and $\delta = 5 \times 10^{-4}$, for the Cauchy problem considered in Example 3.

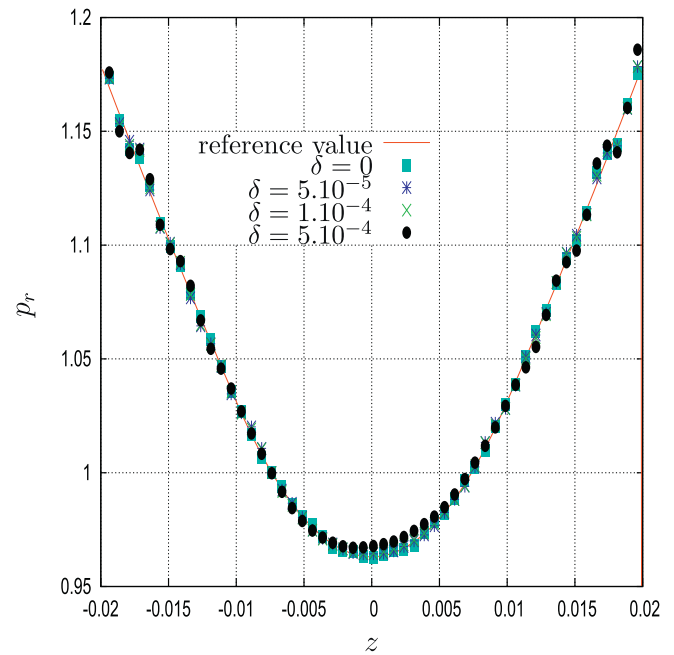because at the end of the boundary part Γ_u some instabilities appear in these reconstructions.

6.5. Reconstructions on Γ_d: Deblurring the noisy data

As the algorithm recomputes a solution on the whole boundary, Fig. 24 gives the reconstruction of the u_r-component on Γ_d and the noisy data u_r^d used ($\delta = 5 \times 10^{-4}$). It can be noted that this
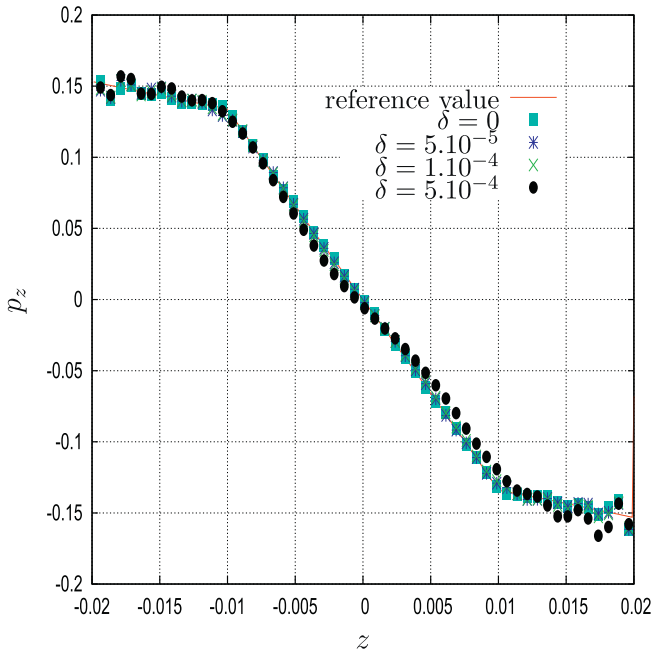
Fig. 23. The reference value and the numerical reconstructions of the axial stress p_z obtained on Γ_u, for $\delta = 5 \times 10^{-5}$, $\delta = 1 \times 10^{-4}$ and $\delta = 5 \times 10^{-4}$, for the Cauchy problem considered in Example 3.

Fig. 25. The reference value and the numerical reconstructions of the ratio R obtained on Γ_u, for $\delta = 5 \times 10^{-5}$, $\delta = 1 \times 10^{-4}$ and $\delta = 5 \times 10^{-4}$, for the Cauchy problem considered in Example 3.
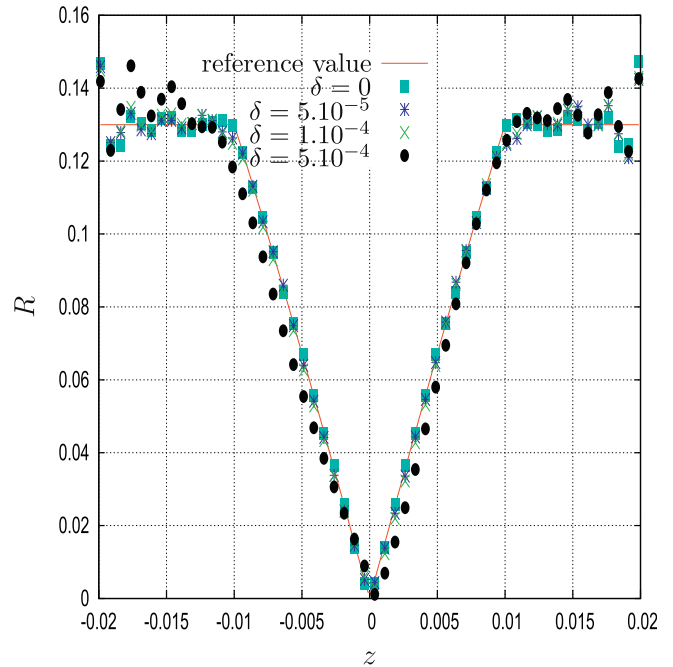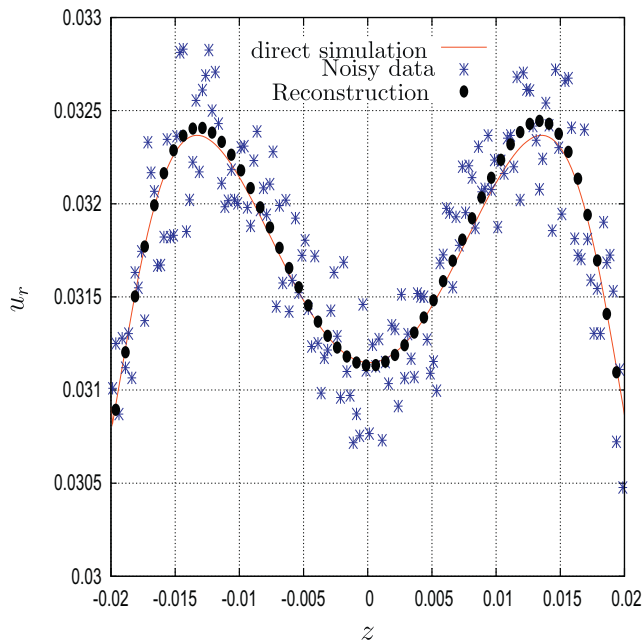
$$R(z) = \left| \frac{p_z(z)}{p_r(z)} \right| \tag{36}$$

The ratio R obtained is quite accurate and allows the extensions of the sliding zones where $R = f$, the extension of the adherence zone where $R < f$ and the value of the friction parameter f to be identified a posteriori with relative precision. It may however be noted that some instabilities appear at the ends of the boundary part Γ_u.

7. Conclusion

This paper introduces an iterative method for solving the Cauchy problem in linear elasticity in axisymmetric situations. This problem consists in recovering missing displacements and forces on some part of a boundary domain from the knowledge of over-specified data on another part of the boundary.

This approach reduces the resolution of the Cauchy problem to the resolution of a sequence of optimization problems under equality constraints. The algorithm reads as a least square fitting. The functional is composed of different terms. Some terms are relaxation terms which represent the gap between the optimal element and the overspecified boundary data. The other term is a regularization term which represents the gap between the optimal element and the previous optimal element. At each step, the optimal element obtained is an exact solution of the equilibrium equations and is close to the overspecified data. The regularization term vanishes when the iterations continue.

Numerical simulations using the finite element method have highlighted the accuracy and robustness of the inverse method to noisy data as well as its ability to deblur noisy data. For all the situations analyzed, it can be observed that the errors in the force reconstructions obtained using the method are higher than those corresponding to the displacements.

On a numerical aspect, further developments will concern the improvement of the inverse method in order to obtain more accurate reconstructions at the ends of the boundary part Γ_u. For the Cauchy problem for the Laplace equation, a first order method

Fig. 24. The numerical reference solution, the noisy data used ($\delta = 5 \times 10^{-4}$) and the numerical reconstruction of the u_r-component of the displacement obtained on Γ_d, for the Cauchy problem considered in Example 3.

reconstruction corresponds to the reference solution obtained with the direct simulation and that the noise in the data has been deleted by the algorithm.

6.6. Identification of the friction coefficient f

Fig. 25 plots, along the boundary part Γ_u, the ratio R between the reconstructions of p_z and those of p_r obtained by the inverse technique:

was introduced in Delvare and Cimetière (2008) to improve the reconstruction of the normal derivatives when the boundary part Γ_u had corners. An extension of this inverse technique to our problem could be very useful.

On the experimental aspect, in further works, the inverse method will be combined with experimental techniques like digital image correlation in order to deal with experimental displacement data.

Acknowledgements

The authors would like to thank the reviewers for their valuable comments.

References

Andrieux, S., Baranger, T.N., 2008. An energy error-based method for the resolution of the Cauchy problem in 3D linear elasticity. Computer Methods in Applied Mechanics and Engineering 197, 902–920.

Bailly, P., Delvare, F., Vial, J., Hanus, J.L., Biessy, M., Picart, D., 2011. Dynamic behavior of an aggregate material at simultaneous high pressure and strain rate: SHPB triaxial tests. International Journal of Impact Engineering 38, 73–84.

Bilotta, A., Turco, E., 2009. A numerical study on the solution of the Cauchy problem in elasticity. International Journal of Solids and Structures 46, 4451–4477.

Bonnet, M., Constantinescu, A., 2005. Inverse problems in elasticity. Inverse Problems 21, R1–R50.

CASTEM 2000, 1998. Code de calcul pour l'analyse de structures par la méthode des éléments finis. Guide d'utilisation. Commissariat l'Energie Atomique, DEN/DM2S/SEMT/LM2S, F-91191 Gif-sur-Yvette, France.

Cimetière, A., Delvare, F., Pons, F., 2000. Une methode inverse avec regularisation evanescente. Comptes Rendus de L Academie des Sciences Paris Tome IIb 328, 639–644.

Cimetière, A., Delvare, F., Jaoua, M., Pons, F., 2001. Solution of the Cauchy problem using iterated Tikhonov regularisation. Inverse Problems 17, 553–570.

Delvare, F., Cimetière, A., Pons, F., 2002. An iterative boundary element method for Cauchy inverse problems. Computational Mechanics 28, 291–302.

Delvare, F., Cimetière, A., 2008. A first order method for the Cauchy problem for the Laplace equation using BEM. Computational Mechanics 41, 789–796.

Delvare, F., Cimetière, A., Hanus, J.L., Bailly, P., 2010. An iterative method for the Cauchy problem in linear elasticity with fading regularization effect. Computer Methods in Applied Mechanics and Engineering 199, 3336–3344.

Ellabib, A., Nachaoui, A., 2008. An iterative approach to the solution of an inverse problem in linear elasticity. Mathematics and Computers in Simulation 77, 189–201.

Forquin, P., Arias, A., Zaera, R., 2007. An experimental method of measuring the confined compression strength of geomaterials. International Journal of Solids and Structures 44, 4291–4317.

Forquin, P., Gary, G., Gatuingt, F., 2008. A testing technique for concrete under confinement at high rates of strain. International Journal of Impact Engineering 35, 425–446.

Gary, G., Bailly, P., Gatuingt, F., 1998. Testing concrete at high strains and high rates of strain. In: 3th International Symposium of Impact Engineering, Singapore.

Hadamard, J., 1923. Lectures on Cauchy's Problem in Linear Partial Differential Equations. Yale University Press, New Haven.

Hansen, P.C., 1992. Analysis of discrete ill-posed problems by means of the L-curve. SIAM Review 34, 561–580.

Koya, T., Yeih, W.C., Mura, T., 1993. An inverse problem in elasticity with partially overspecified boundary conditions. II. Numerical details. Transactions of the ASME. Journal of Applied Mechanics 60, 601–606.

Kubo, S., 1988. Inverse problems related to the mechanics and fracture of solids and structures. JSME International Journal Series I 31, 157–166.

Maniatty, A., Zabaras, N., Stelson, K., 1989. Finite element analysis of some elasticity problems. Journal of Engineering Mechanics Division ASCE 115, 1302–1316.

Marin, L., Elliott, L., Ingham, D.B., Lesnic, D., 2001. Boundary element method for the Cauchy problem in linear elasticity. Engineering Analysis with Boundary Elements 25, 783–793.

Marin, L., Lesnic, D., 2002a. Regularized boundary element solution for an inverse boundary value problem in linear elasticity. Communications in Numerical Methods in Engineering 18, 817–825.

Marin, L., Lesnic, D., 2002b. Boundary element solution for the Cauchy problem in linear elasticity using singular value decomposition. Computer Methods in Applied Mechanics and Engineering 191, 3257–3270.

Marin, L., Elliott, L., Ingham, D.B., Lesnic, D., 2002a. Boundary element regularization methods for solving the Cauchy problem in linear elasticity. Inverse Problems in Engineering 10, 335–357.

Marin, L., Hao, D.N., Lesnic, D., 2002b. Conjugate gradient-boundary element method for the Cauchy problem in elasticity. Quarterly Journal of Mechanics and Applied Mathematics 55, 227–247.

Marin, L., Lesnic, D., 2003. BEM first-order regularization method in linear elasticity for boundary identification. Computer Methods in Applied Mechanics and Engineering 192, 2059–2071.

Marin, L., Lesnic, D., 2004. The method of fundamental solutions for the Cauchy problem in two-dimensional linear elasticity. International Journal of Solids and Structures 41, 3425–3438.

Marin, L., 2005. A meshless method for solving the Cauchy problem in three-dimensional elastostatics. Computers and Mathematics with Applications 50, 73–92.

Marin, L., Lesnic, D., 2005. Boundary element-Landweber method for the Cauchy problem in linear elasticity. IMA Journal of Applied Mathematics 18, 817–825.

Marin, L., 2009. The minimal error method for the Cauchy problem in linear elasticity. Numerical implementation for two-dimensional homogeneous isotropic linear elasticity. International Journal of Solids and Structures 46, 957–974.

Marin, L., Johansson, B.T., 2010a. A relaxation method of an alternating iterative algorithm for the Cauchy problem in linear isotropic elasticity. Computer Methods in Applied Mechanics and Engineering 199, 3179–3196.

Marin, L., Johansson, B.T., 2010b. Relaxation procedures for an iterative MFS algorithm for the stable reconstruction of elastic fields from Cauchy data in two-dimensional isotropic linear elasticity. International Journal of Solids and Structures 47, 3462–3479.

Schnur, D., Zabaras, N., 1990. Finite element solution of two-dimensional elastic problems using spatial smoothing. International Journal for Numerical Methods in Engineering 30, 57–75.

Tikhonov, A.N., Arsenin, V.Y., 1977. Solution of Ill-posed Problems. John Wiley and Sons, New York.

Yeih, W.C., Koya, T., Mura, T., 1993. An inverse problem in elasticity with partially overspecified boundary conditions. I. Theoretical Approach, Transactions of the ASME Journal of Applied Mechanics 60, 595–600.

Zabaras, N., Morellas, V., Schnur, D., 1989. Spatially regularized solution of inverse elasticity problems using the BEM. Communications in Applied Numerical Methods 5, 547–553.